FIBROPOROUS POLYTETRAFLUOROETHYLENE MODIFIED OF GOLD AND SILVER NANOPARTICLES BY SUPERCRITICAL CARBON DIOXIDE AND METAL-VAPOR SYNTHESIS

L.N. Nikitin[1], A.Yu. Vasilkov[1,2], A.V. Naumkin[1], S.S. Abramchuk[1], Yu.N. Bubnov[1], E.M. Tolstopyatov[3], P.N. Grakovich[3], S.K. Rakhmanov[3]

[1]*Nesmeyanov Institute of Organoelement Compounds, Russian Academy of Sciences, Vavilova St., 28, Moscow, 119991 Russia, lnik@ineos.ac.ru*
[2]*Department of Chemistry, Lomonosov Moscow State University, Leninskie gory, Moscow, 119992 Russia;*
[3]*Biely Institute of Mechanics of Metal-Polymer Systems, National Academy of Sciences of Belarus, Gomel, 246050 Belarus*

Abstract

A combined approach to the synthesis of functional nanocomposite materials based on fibroporous polytetrafluoroethylene (PTFE) prepared by the CO_2 laser irradiation of the block PTFE sample (teflon-4) has been developed. Fibroporous materials (FPM) such as cotton and felt were modified by supercritical carbon dioxide treatment to create nano- and micropores in the surface layers of FPM fibers. The gold and silver-containing fibroporous nanocomposites have been obtained by processing the nanostructured FPM with the organosols of the metal nanoparticles in isopropanol prepared by metal-vapor synthesis. The composition and structure of the metalcontaining fluoropolymers have been investigated by X-ray analysis and electron microscopy.

Introduction

Polytetrafluoroethylene (PTFE) refers to biostable polymers and, due to its high chemical inertness and hydrophobicity, is widely used in medicine [1]. The production of PTFE in the form of fibroporous materials (FPM) [2–5] has considerably expanded the range of problems in which it can be used in biological barrier elements, obturators, and isolating and dressing materials. These materials are rather effective in purifying gases from water, oil, and acid aerosols. The further expansion of the scope of the PTFE applications can be reached by modifying FPM with metal nanoparticles in order to provide them with antibacterial, magnetic, and other properties. By introducing the necessary amount of metal nanoparticles and by effective stabilization in the surface layers, the porosity of materials is increased. One of method to form the porous structure in PTFE can be its processing in the supercritical carbon dioxide (sc CO_2) by pulse modification (PM) [6]. The combined usage of metal-vapor synthesis (MVS) and PM to obtain mono- and bimetallic nanoparticles of different compositions and structures [7–9] has allowed the creation of new hybrid nanomaterials on the basis of a powder material (ultradisperse PTFE [10]).

In this work, the complex technological approach to obtain metalcontaining nanocomposites based on a combination of three original techniques (laser ablation of PTFE with the formation of fibroporous materials, their pulse processing in sc CO_2, and modification with gold and silver nanoparticles obtained by MVS) is presented.

Experimental

Fibroporous PFFE was obtained by processing the block polymer by the continuous radiation of the CO_2 laser in vacuum [2, 3]. The LGN_703 laser with a radiation power of 40–45 W and the LGN-709 laser with a radiation power of 90–120 W were used. A simplified scheme of the ablation chamber is given in Fig. 1. PTFE of the F-4 grade (OAO Kirovo-Chepetskii khimicheskii kombinat) was used as the initial target material.

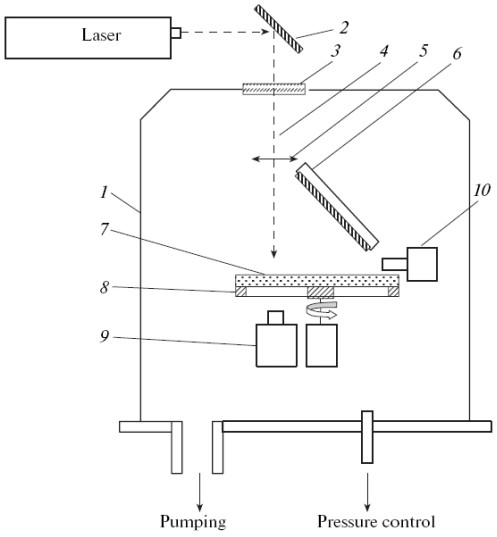

Fig. 1. Scheme of the main block of the laser ablation setup. (*1*) vacuum chamber; (*2*) mirror; (*3*) vacuum_dense window for the radiation input; (*4*) passage of the laser beam; (*5*) lens; (*6*) a substrate to collect ablation products; (*7*) PTFE target; (*8*) target holder; (*9*) gauge of the meter of the radiationpower; (*10*) web-chamber.

The setup scheme and techniques of working with sc CO_2 are given in [11, 12]. Polymer (3–5 g) in an extraction container was placed in an autoclave with a volume of 12 cm^3, which was pressurized and blown through for 2–3 min with carbon dioxide to remove air and water vapors. After hermetic sealing the autoclave was temperature-controlled at 90°C and a CO_2 pressure of 90 MPa was created. After the exposition of polymer in these conditions for 3 h, the fast decompression of the autoclave with was performed a release velocity of CO_2 of 5 cm^3/s. A pulse (with a quick release of CO_2) modification of polymers sc CO_2 was consequently performed twice. The surface area of porous FPMs after this processing measured by the Brunauer-Emmett-Teller (BET) method increased by 7.5% from 2.7 to 2.9 m^2/g. In experiments, CO_2 with a purity grade of about 99.995% (GOST 8050-85) was used.

Nanocomposites on the basis of gold and silver were obtained by modifying fluoropolymers processed with sc CO_2 by metal organosols in isopropanol obtained by MVS [6–9]. Metals were evaporated in a vacuum of 10^{-4} mm Hg: gold (99.99%) from a tungstic rod and silver (99.99%) from a tantalum boat. Isopropanol (99.8% Fluka) was dried and distilled over zeolites in an atmosphere of purified. Before synthesis, it was degassed in a vacuum by the alternation of freeze-defreeze cycles. Metal and isopropanol vapors were simultaneously condensed on the walls of a glass reactor with a volume of 5 l cooled by liquid nitrogen. In typical experiments, the molar reagent metal-to-isopropanol ratio varied within the limits of 1 : 300–500. After the synthesis was terminated, cooling was stopped, cocondensate was heated up until it melted, and the organosol obtained was used to impregnate in vacuum fluoropolymer kept in the Schlenk flask. The excess of the organosol was deleted, and the remaining product was dried in vacuum at 100°C.

X-ray photoelectron spectra were recorded on a Kratos XSAM800 spectrometer (Great Britain). A magnesium anode with the characteristic radiation energy MgK_α = 1253.6 eV was used as an excitation source. The spectrometer energy scale was calibrated by a standard technique with the following bonding energy values: Cu 2p3/2, 932.7 eV; Ag 3d5/2, 368.3 eV; and 4f7/2, – 84.0 eV [13]. The surface charge was compensated according to the F 1s peak with the attributed energy of 689.7 eV corresponding to PTFE [14]. A quantitative analysis was performed on the basis of the element sensitivity coefficients (ESC) from a package of applied programs.

Microscopic studies of nanocomposites were performed on a LEO 912 , OMEGA transmission microscope (Zeiss, Germany) and a Hitachi S-520 scanning microscope (Japan). Before scanning samples on a raster electron microscope, the film surface was covered by a 15 nm thick layer of gold (IB-3 Ion Coater, Eiko Engineering, Japan).

Diffraction measurements were performed on Bruker D8 Advance diffractometer (λ[CuK_α])] =1.54184 E in the interval of 2θ angles from 2 to100 with a step of 0.02 and exposition time of 10 s per step at room temperature.

Results and Discussion

Experiments on the influence of the continuous radiation of the CO_2 laser on PTFE have shown that the most unique features of this polymer are manifested not only at ultra short pulse impacts [15], but also upon long-term continuous irradiation [2]. Laser ablation of polymers is a complex process including [16] optical interaction; heat transfer; phase transformations; the thermal destruction of macromolecules; the diffusion of low-molecular decomposition products in the zone of the laser impact; thermo-chemical reactions in the irradiated polymer layer and in the medium of the evaporated decomposition polymer product; and the evaporation of the fragments of macromolecules, which, as a result of destruction, have reached a weight capable of sublimation without decomposition at the temperature on the surface crater.

The results of the ablation experiments on most polymers with the radiation of the CO_2 were predicted on the basis of data on thermal destruction in vacuum. Among the polymers produced on the industrial basis, only PTFE revealed abnormal behavior [2, 17, 18]. The impact of the radiation of the CO_2 laser on PTFE leads to the formation of ablation products in two aggregate states in the form of gas and in the form of microscopic flows of the melt extracted by the gas flow. In the stationary mode of the energy impact, the bridges of the melt between microcraters under the action of the intensive flow of hot gas are broken off and extended along the flow. At low radiation intensity, the fiber is thrown to the crater periphery and, remaining connected with the target on its border, forms the cotton wool of PTFE. At the high radiation intensity, the fibers come off the target and are carried away by the flow of the destruction products. When getting to the firm surface, they are alloyed with each other in their place of a contact, forming a layer of felt (Fig. 2).

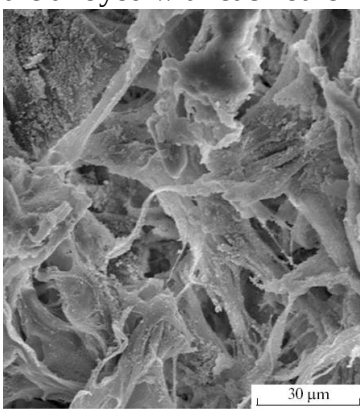

Fig. 2. Electron microphoto of the structure of the surface of felt from PTFE.

As a result of these impacts, the sites with the changed chemical structure are formed in the surface fiber layer [18] shown by X-ray photoelectron spectrtoscopy (XPS). In the C 1spectrum of fibers, four states corresponding to the CF_2–C · F_2–CF_2 (292.5 eV), CF_2–C ·F–CF_2 (290.4 eV), C–C · F_2–C (290.4 eV), C–C · F–C (2881 eV), and C–C, H (285.0 eV) groups and, in the F ls spectrum, two states with the bonding energies of 689.7 and 688.7 eV are singled out. A quantitative XPS analysis gives the composition C0.36F0.66 close to the stoichiometric formula of PTFE, CF_2. The TGA study has shown that the thermal stability of the initial PTFE and laser ablation products is the same and the temperature of the loss of 5% weight is 510°C.

The IR_spectra of the initial PTFE and fiber material are identical, except for the site responsible for the fluctuations in the amorphous and crystal states. Felt has two levels of porous structure: one is formed by interfiber intervals and the second is determined by the structure of a fiber and includes internal nanopores up to 40 nm. The separate fibers, mostly felt, are punched surface nanopores as seen in Fig. 2.

An analysis of the obtained results has allowed us to assume that the porosity of the second level can be developed to an even greater degree at processing in sc CO_2 and will have a higher affinity to metal nanoparticles obtained by MVS.

The FPM yield is 10–15% under the standard irradiation conditions and increases up to 24–26% with the increasing temperature when additionally heating the target to 680 K. The laser radiation intensity strongly influences the form of fibers. At the radiation intensity of 0.6 MW/m^2, the fibers mainly have smooth surface. The increase in the intensity up to 50–100 MW/m^2 leads to fibers with a lot of branchings, which are apertures of the irregular form (Fig. 2). According to X-ray diffraction measurements of various process conditions of [16, 18], the crystal state of the fibrous fraction of the ablation products is identical to that of industrial PTFE.

Modifying sc CO_2-processed FPM with gold and silver organosols results in homogeneous material with a metal content in the surface layer from 2 up to 9 wt%. This composition is recorded by XPS. However, the microanalysis of the material shows the considerably lower metal content within the limits of 0.4–1.1 wt %. This indicates that the nanoparticles are basically stabilized in the micro- and nanocavities of the near-surface layer (up to 50 E), which is accessible to the XPS diagnostics.

TEM data of the sc CO_2 processed fiber reveal only the nanocracks and "tension bars" irregularly located on the surface of the material. The distribution of silver particles on the sample surface (Fig. 3) is of a bimodal character and is characterized by particles with an average size of 4 and 30 nm.

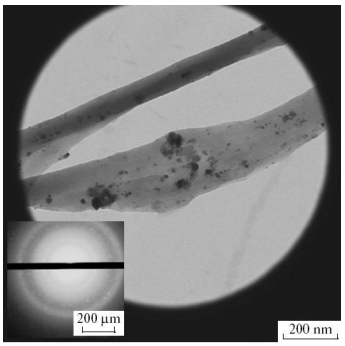

Fig. 3. TEM microphoto of the silver_containing felt fiber. In the left bottom corner is its electronogram.

The analysis of the nano-metal formations with the sizes from 20 to 40 nm has shown that they have a structure of a "bunch of grapes" which combines finer particles. The presence of large particles may be due to the presence of microcavities capable of accumulating nanoparticles from the organosol in the initial material. After the deposition of Ag on the fiber, in addition to the peaks characteristic for PTFE and Ag, the peaks characteristic for oxygen are observed in the spectrum.

The quantitative XPS analysis gives the structure $C_{0.42}F_{0.54}O_{0.03}Ag_{0.01}$. The application of the positive and negative displacement voltage (U_{dis}) of 7 V to the sample results in the displacement of the F 1 s and F KLL peaks by 2 eV to the higher and lower values of the bonding energy, respectively, without any change in the form of spectral lines. This indicates that there are no physical or chemical heterogeneities connected with fluorine. It also confirms the slight change in the Auger-parameter within the limits of the experimental error. After the deposition of Ag s, the low energy shoulder in the F 1s spectra disappears, reflecting the equalization of the electron potential at the surface close to the fluorine atoms. A similar phenomenon is observed after the deposition of gold nanoparticles on felt as well. The form of the Ag 3d spectral line does not vary when *U*dis is applied. Regardless of the polarity of the applied voltage, the Ag 3d5/2 peak is displaced by 0.3 eV to the higher energies. However, in the C 1s and O 1s spectra, both the form of lines and the position of peaks change when U_{dis} is applied (Fig. 4).

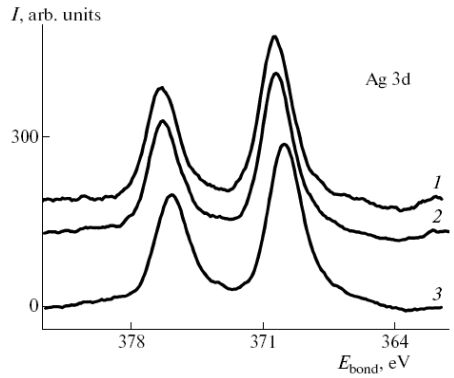

Fig. 4. Photoelectron Ag 3d spectra of the Ag/fiber sample recorded at *U*dis = 0 (*1*), –7 (*2*) and +7 V (*3*). Spectra are given taking into account the surface charging and normalized to the peak with the maximal intensity.

This indicates the presence of regions differing in the conductivity and emission properties and, accordingly, structure. The changes in the energy position of the Ag 3d5/2 peak, depending on the applied displacement voltage with the constant form of the spectral line, indicate the presence of a charge on the Ag particles. The shift of the Ag 3d5/2 peak to higher energies can indicate both a positive charge on the Ag particles and a dimensional effect. In the Ag niello spectra, the weak dependence of the full width at the half-height (FWHH) of the Ag 3d5/2 peak on U_{dis} is observed with the constant peak position (after taking into account the *U*dis value). The minimal FWHH value of 1.3 eV is observed at *U*dis = 0 V and the maximal one of 1.5 eV at U_{dis} = –7 V. At U_{dis} = 7 V, the FWHH value is 1.4 eV. In this case the spectral broadening occurs both at the positive and negative U_{dis} value. This indicates

the presence of a charge on the Ag particles which, apparently, leads to the above changes in the Ag 3d spectrum.

The Ag 3d5/2 shift with respect to the position of the reference Ag sample of 1.5 eV is mainly due to the differential charging of the sample surface and is not the result of the chemical interaction between Ag atoms and PTFE. The differential charging is manifested in the broadening of the Ag 3d7/2 peak by 0.9 eV with respect to the niello peak with FWHH of 1.3 eV at *U*dis of 0 V. The approximately twice as much decrease in the intensity of the peak with the energy of 688.7 eV in the F 1s spectrum may be due to the interaction between Ag and F. One can see that, upon a variation of the displacement voltage, the bonding energies of all peaks with respect to the F 1s peak change. This also indicates the heterogeneity of the sample because, in case of the homogeneous sample, the difference of the bonding energies F 1s– C 1s and others should not depend on the applied displacement voltage and be constant.

The introduction of Au nanoparticles leads to a displacement of the main peak in the C 1s spectrum and to an increase in its FWHH by 0.1 and 0.3 eV with respect to the analogous peak in the spectra of the initial PTFE fiber and the Au/fiber sample with its FWHH of 2.8 eV. Thus, the shift of the Au 4f7/2 peak with respect to the u foil peak is of 0.9 eV and FWHH is of 2.4 eV. In the case of the u foil, the FWHH value is 1.6 eV. Figure 5 shows the corresponding Au 4f spectra. The shift and FWHH values indicate the manifestation of the dimensional effect.

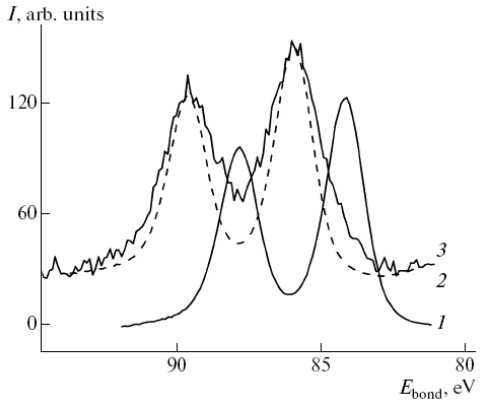

Fig. 5. Photoelectron Au 4f spectra of the Au foil (*1*), after the displacement by 0.9 eV (*2*), and of the Au/fiber sample (*3*).

Conclusions

A complex technique to obtain gold- and silvercontaining nanocomposite materials on the basis of fibroporous PTFE by the laser ablation of Teflon-4 was developed. It was established that the fluoropolymer fibers have a chemical composition close to that of the initial PTFE. Processing of the fibroporous fluoropolymer in supercritical carbon dioxide by PM leads to an 8% increase in the specific surface and the formation of nanopores in the near-surface layer. The porous structure of fluoromaterials after sc CO_2 processing effectively stabilizes the gold and silver particles with average sizes of 4 and 30 nm obtained by MVS.

Acknowledgments

This work was supported by the Russian Foundation for Basic Research (projects no. 08-03-00294, 08-03-90012, 08-03-12152, 09-03-91227 and 10-03-90030), the Russian Academy of Sciences (the project under the set of the Branch ChSM programs of the Russian Academy of Sciences “The Creation of New Metal, Ceramic, Glass, Polymeric, and Composite Materials” and Presidium RAS (Programme P-21).

REFERENCES

1. K. Z. Gumargalieva, G. E. Zaikov, Yu. V. Moiseev, Macrokinetic Aspects of the Biocompatibility and Biodegradation of Polymers, Usp. Khim., 1994, vol. 63, No.10, pp. 906–921.
2. A. M. Krasovskii, E. M. Tolstopyatov, Use of Laser Radiation for the Formation of Polymer Films in Vacuum on the Solid Surface, Poverkhnost, 1985, No. 1, pp. 143–149.
3. A. M. Krasovskii, E. M. Tolstopyatov, P. N. Grakovich, L. F. Ivanov, The Method for Preparing a Cotton from Polytetrafluoroethylene, USSR Inventor’s Certificate, 1986, No. 1 461 052.
4. A. M. Krasovskii, E. M. Tolstopyatov, Production of Thin Films by Sputtering of Polymers in Vacuum (Nauka i Tekhnika, Minsk, 1989, [in Russian].

5. E. M. Tolstopyatov, L. F. Ivanov, P. N. Grakovich, A. M. Krasovsky, Destruction of Polytetrafluoroethylene under the Action of Carbon Dioxide Laser Radiation at Low Pressure, Proc. SPIE—Int. Soc. Opt. Eng. 1998, 3343 (Part 2), pp. 1010–1017.
6. A. Vasil'kov, A. Naumkin, L. Nikitin, I. Volkov, V. Podshibichin, G. Lisichkin, Ultrahigh Molecular Weight Polyethylene Modified with Silver Nanoparticles Prepared by Metal-Vapour Synthesis, AIP Conf. Proc. 2008, vol. 1042, pp. 255–257.
7. S. A. Nikolaev, V. V. Smirnov, I. P. Beletskaya, A. Yu. Vasil'kov, A. V. Naumkin, L. A. Tyurina, Synergism of the Catalytic Action of Au–Ni Nanocomposites in Allyl Isomerization of Allylbenzene, Ross. Nanotekhnol. 2007, vol. 2 No. (9–10), pp. 58–66.
8. A. Yu. Vasil'kov, S. A. Nikolaev, V. V. Smirnov, A. V. Naumkin, I. O. Volkov, V. L. Podshibichin, An XPS Study of the Synergetic Effect of Gold and Nickel Supported on SiO_2 in the Catalytic Isomerization of Allylbenzene, Mendeleev Commun. 2007, vol. 17, No. 5, pp. 268–270.
9. I. P. Suzdalev, Yu. V. Maksimov, A. Yu. Vasil'kov, A. V. Naumkin, V. L. Podshibikhin, I. O. Volkov, Electronic and Magnetic Properties of Au–Fe Cluster Nanocomposites Prepared by a Sequential Solvated Metal Vapor Dispersion Process, Ross. Nanotekhnol. 2008, vol. 3, No. (1–2), pp. 76–81.
10. L. N. Nikitin, A. Yu. Vasil'kov, A. R. Khokhlov, V. M. Bouznik, Metal–Polymer Composites Manufactured via Metal Vapor Synthesis Using Supercritical Carbon Dioxide, Dokl. Phys. Chem. 2008, vol. 422 (Part 2), pp. 256-260.
11. M. O. Gallyamov, L. N. Nikitin, A. Yu. Nikolaev, A. N. Obraztsov, V. M. Bouznik, A. R. Khokhlov Formation of Superhydrophobic Surfaces by the Deposition of Coatings from Supercritical Carbon Dioxide, Colloid J., 2007, vol. 69, No. 4, pp. 411–424.
12. L. N. Nikitin, A. Yu. Nikolaev, E. E. Said-Galiev, A. I. Gamzazade, A. R. Khokhlov, Formation of Porosity in Polymers with the Use of Supercritical Carbon Dioxide, Sverkhkrit. Flyuidy, Teor. Prakt. 2006, vol. 1, No. 1, pp. 77–88.
13. C. D. Wagner, A. V. Naumkin, A. Kraut_Vass, J. W. Allison, C. J. Powell, J. R. Rumble, Jr., NIST X-Ray Photoelectron Spectroscopy Database, Version 3.5 (National Institute of Standards and Technology, Gaithersburg, MD, United States, 2003); http://srdatanist.gov@xps.
14. G. Beamson, D. Briggs, High_Resolution XPS of Organic Polymers (Wiley, Chichester, 1992).
15. A. A. Serafetinidis, M. I. Makropoulou, C. Skordoulis, A. R. Kar, Ultra-Short Pulsed Laser Ablation of Polymers, Appl. Surf. Sci. 2001, vol. 180, pp. 42–56.
16. E. M. Tolstopyatov, Physical Mechanisms of the Dissociative Formation of Thin Polymer Coatings, Doctoral Dissertation in Technical Sciences (Belyi Metal Polymer Research Institute of the National Academy of Sciences of Belarus, Gomel, 2007).
17. E. M. Tolstopyatov, P. N. Grakovich, L. F. Ivanov, I. L. Ryabchenko, On the Mechanism of Formation of Fibers upon Laser Ablation of Polytetrafluoroethylene, Vopr. Khim. Khim. Tekhnol., 2002, No. 3, pp. 128–131.
18. E. M. Tolstopyatov, Ablation of Polytetrafluoroethylene Using a Continuous CO_2 Laser Beam, J. Phys. D: Appl. Phys. 2005, vol. 38, pp. 1993–1999.